12-1984

Kinetics of the Formation of the Nickel(II) Complex with N, N' -Dimethylethylenediaminediacetic Acid and the Metal Exchange Reaction between N,N'-Dimethylethylenediaminediacetatonickel(II) and Copper(II)

Roger A. Karel

KINETICS OF THE FORMATION OF THE NICKEL(II) COMPLEX WITH N,N'-DIMETHYLETHYLENEDIAMINEDIACETIC ACID AND THE METAL EXCHANGE REACTION BETWEEN N,N'-DIMETHYL-ETHYLENEDIAMINEDIACETATONICKEL(II) AND COPPER(II)

by

Roger A. Karel

A Thesis
Submitted to the
Faculty of The Graduate College
in partial fulfillment of the
requirements for the
Degree of Masters of Arts
Department of Chemistry

Western Michigan University
Kalamazoo, Michigan
December 1984

KINETICS OF THE FORMATION OF THE NICKEL(II) COMPLEX WITH N,N'-DIMETHYLETHYLENEDIAMINEDIACETIC ACID AND THE METAL EXCHANGE REACTION BETWEEN N,N'-DIMETHYLETHYLENEDIAMINEDIACETATONICKEL(II) AND COPPER(II)

Roger A. Karel, M.A.

Western Michigan University, 1984

The kinetics of the reaction of aquonickel(II) ion with N,N'-dimethylethylenediaminediacetic acid has been studied at 25°C and 0.1M ionic strength over a pH range of 6.0 to 9.3 using stopped-flow techniques. Formation reactions in all cases were first-order in Ni(II) and in ligand. The formation rate constant for the protonated and unprotonated species were evaluated and compared to their theoretical value. The rate-determining step is shown to be ring closure. A comparision of this system with other studies involving complexation of nickel(II) confirm the magnitude of the internal conjugate base effect and also shows a correlation between the internal conjugate base rate enhancement and the structural environment of the nitrogen donor atom.

The exchange reaction between copper(II) and N,N'-dimethylethylenediaminediacetatonickelate(II) was studied at 25°C over a four fold variation in copper concentration with an ionic strength of 1.25M and a pH of 3.26. The reaction was shown to be first-order in NiDMEDDA and zero-order in copper. This zero-order dependence shows the inablity of DMEDDA to unwrap from nickel and twist into a conformation suitable for bonding to copper prior to the rate limiting step.

ACKNOWLEDGEMENTS

To Professor Ralph K. Steinhaus, my research advisor, I wish to express my sincere appreciation for his expert guidance and support during the completion of this work. Thanks are also given to the faculty of the chemistry department and especially to the members of the author's committee, Dr. Dean W. Cooke and Dr. H. Dale Warren.

To my wife Nancy, and to my children Amanda and Matthew, I am especially indebted for their kindness and support. I also wish to express a special appreciation to my parents as well as to my wife's mother for their encouragment throughout my graduate work.

Roger A. Karel

INFORMATION TO USERS

This reproduction was made from a copy of a document sent to us for microfilming. While the most advanced technology has been used to photograph and reproduce this document, the quality of the reproduction is heavily dependent upon the quality of the material submitted.

The following explanation of techniques is provided to help clarify markings or notations which may appear on this reproduction.

1. The sign or "target" for pages apparently lacking from the document photographed is "Missing Page(s)". If it was possible to obtain the missing page(s) or section, they are spliced into the film along with adjacent pages. This may have necessitated cutting through an image and duplicating adjacent pages to assure complete continuity.

2. When an image on the film is obliterated with a round black mark, it is an indication of either blurred copy because of movement during exposure, duplicate copy, or copyrighted materials that should not have been filmed. For blurred pages, a good image of the page can be found in the adjacent frame. If copyrighted materials were deleted, a target note will appear listing the pages in the adjacent frame.

3. When a map, drawing or chart, etc., is part of the material being photographed, a definite method of "sectioning" the material has been followed. It is customary to begin filming at the upper left hand corner of a large sheet and to continue from left to right in equal sections with small overlaps. If necessary, sectioning is continued again–beginning below the first row and continuing on until complete.

4. For illustrations that cannot be satisfactorily reproduced by xerographic means, photographic prints can be purchased at additional cost and inserted into your xerographic copy. These prints are available upon request from the Dissertations Customer Services Department.

5. Some pages in any document may have indistinct print. In all cases the best available copy has been filmed.

University Microfilms International
300 N. Zeeb Road
Ann Arbor, MI 48106

KAREL, ROGER ALLEN

KINETICS OF THE FORMATION OF THE NICKEL(II) COMPLEX WITH N,N'-DIMETHYL ETHYLENEDIAMINEDIACETIC ACID AND THE METAL EXCHANGE REACTION BETWEEN N,N'-DIMETHYLETHYLENEDIAMINE DIACETATONICKEL(II) AND COPPER(II)

WESTERN MICHIGAN UNIVERSITY M.A. 1984

TABLE OF CONTENTS

TABLE OF CONTENTS cont.

LIST OF TABLES

LIST OF FIGURES

LIST OF ABBREVIATIONS

BPEDA	N,N'-bis-(2 picolyl)ethylenediamine
CHES	cyclohexylaminoethane sulfonic acid
DBEDA	N,N'-dibenzyethylenediamine
DMEDDA	N,N'-dimethylethylenediaminediacetic acid
EDDA	ethylenediaminediacetic acid
gly	glycine
HEPES	N-2-hydroxyethylpiperzine-N'-2-ethanesulfonic acid
ICB	internal conjugate base
MES	2(N-morpholino)ethane sulfonic acid
NiDMEDDA	N,N'-dimethylethylenediaminediacetato-nickelate(II)
NiEDDA	ethylenediaminediacetatonickelate(II)
sar	sarcosine
TAPS	tris (hydroxymethyl)methylaminopropane sulfonic acid
TKED	N,N,N',N'-tetrakis(2-hydroxyethyl)ethylenediamine
Trien	triethylenetetramine

INTRODUCTION

The development of techniques for the kinetic study of rapid reactions has resulted in an extensive accummulation of rate data for reactions of the type

$$M(H_2O)_6^{n+} + L^{b-} \longrightarrow M(H_2O)_5L^{(n-b)+} + H_2O \qquad (1)$$

The results of these systems have been reviewed by several authors (1-3). Because many of its reactions proceed at rates accessible to stopped-flow investigations, hexaaquonickel(II) has been used extensively as a substrate for these studies. The behavior which has been observed for nickel(II) is typical of that for a large class of aquometal ions. The characteristic kinetic features of these reactions can be summmarized briefly. (i) The rate law for the formation of $M(H_2O)_5L$ is second-order over all, first-order in metal ion, and first-order in ligand. (ii) For a given metal ion, large variations in formation rates can be observed with different ligands. In general, ligands bearing a large negative charge react rapidly, while those bearing a less negative charge react more slowly. Ligands having the same charge tend to react at the same rate; such variations as are observed fail to correlate with expected relative nucleophilicities. (iii) For a range of metal ions, ligand-substitution rates parallel the rates of water exchange.

These observations are accounted for by a general dissociative mechanism formulated by Eigen (4) which has been sucessful in predicting experimentally determined rate constants for many 1:1 complex formation reactions involving a varity of ligands. For the reaction of

aquated Ni^{2+} with a bidentate ligand, the Eigen-Tamm mechanism is written as follows

$$Ni(H_2O)_6^{2+} + (L\text{-}L)^{n-} \xrightarrow{K_{os}} \underset{A}{Ni(H_2O)_6 \cdot (L\text{-}L)^{2-n}} \quad (2)$$

$$A \underset{k_{-1}}{\overset{k_1}{\rightleftharpoons}} \underset{B}{(H_2O)_5Ni\text{-}L\text{-}L^{2-n}} + H_2O \quad (3)$$

$$B \underset{k_{-2}}{\overset{k_2}{\rightleftharpoons}} \underset{C}{(H_2O)_4Ni\begin{array}{l}L\\|\\L\end{array}} + H_2O \quad (4)$$

In the above reaction sequence, $(L\text{-}L)^{n-}$ represents the bidentate ligand whereas, $Ni(H_2O)_6^{2+}$ is the aquated nickel ion in solution. The initial step (equation 2) represents a diffusion controlled rapid pre-equilibrium of reactants to form an outer-sphere complex A. The association equilibrium constant for species A is represented by K_{os}. In equation 3, species A loses a water molecule from the inner coordination sphere of the nickel(II) ion, and this process is immediately followed by coordination of ligand L-L to give the monocoordinated species B. The forward rate constant for this step (equation 3) is denoted

$$k_1 = k^{Ni\text{-}H_2O} \quad (5)$$

This latter equation describes water exchange at nickel. The reverse process in equation 3 involves rupture of the Ni-L bond to form A, and the corresponding reverse rate constant is called k_{-1}. The final step (equation 4) describes the loss of a second coordinated water molecule from the inner coordination sphere of species B, followed by ring closure of L-L to form the binary complex, species C. The forward and reverse rate constants for the last step are given by k_2 and k_{-2} respectively.

In order to derive a rate expression for product formation using the Eigen-Tamm mechanism, three assumptions are normally made:

1) the pre-equilibrium (equation 2) is rapid
2) the monocoordinated species B is a steady state intermediate
3) k_{-2} is small and maybe neglected

Using these three assumptions, the derived rate law for product formation is written

$$\frac{d[C]}{dt} = \frac{K_{os}k_1k_2}{(k_{-1}+k_2)}[Ni(H_2O)_6^{2+}][(L_2)^{n-}] \qquad (6)$$

Thus the kinetic behavior is expected to be first-order with respect to each reactant, with an overall second-order rate constant k_{Ni}^{L} given by

$$k_{Ni}^{L} = \frac{K_{os}k_1k_2}{(k_{-1}+k_2)} \qquad (7)$$

Steps following the first loss of a coordinated water molecule from the metal ion in the outer-sphere complex are usually rapid so that the first such metal-water bond rupture represents the rate-determining step, even for reactions of multidenate ligands which involve subsequent bonding steps (5). Under these conditions, the formation rate constant, k_M^L, can be expressed as

$$k_M^L = K_{os}k^{M-H_2O} \qquad (8)$$

For such systems the reaction intermediate preceeding water loss is a true "ion pair," and the value of the association equilibrium constant, K_{os}, can be calculated

(5,6) with a fair degree of accuracy from diffusion equations (7,8). The rate constant for metal-water bond rupture, k^{M-H_2O}, has been determined independently for metal ions from temperature-jump (4,9,10), sound absorption (4), and nuclear magnetic resonance measurments (4,11). Therefore, the formation rate constant k_M^L, in many instances, can be approximated from a priori calculation using equation 8. In this manner comparison can be made between theoretical and experimental rate constant values as a test for the applicability of the dissociative mechanism (9). The constancy of formation rate constants for reactions involving a series of ligands of the same charge reacting with a specific aquometal ion also serves to support this mechanism (4,5).

Instances in which the theoretical and experimental rate constants differ have led to the postulation of ligand effects to explain these differences.

Studies with highly basic N-substituted diamines (12,13) have shown formation rate constants which markedly exceed the theoretical values. To account for this apparent deviation, a modification of the general mechanism as given in equations 2, 3, and 4 is postulated (9) wherein a basic donor atom of the reacting multidenate ligand forms a hydrogen bond to a coordinated water molecule, thereby stabilizing the outer-sphere.intermediate and labilizing subsquent water loss. As a result, the multidentate ligand promotes its own coordination. This "internal conjugate base" (ICB) mechanism has been observed in the formation reactions of Ni(II) ion with a variety of multidentate ligands including 2-aminomethylpyridine (14), N,N'-dibenzyethylenediamine (DBEDA), N,N'-bis-(2-picolyl)ethylenediamine (BPEDA) (15), and triethylenetetramine (trien) (16).

In contrast to the rate enhancement of the ICB

effect, studies of the reaction of Ni(II) ion with N-alkyl-substituded monoamines (17) and N-alkyl-substituted ethylenediamines (12) have shown that steric constraints exert a pronounced rate-depression effect on the formation rate constant as a result of blocking the site of coordination.

Turan's study of N-methyl substituted ethylenediamine (18) demonstrated that for appropriate ligands, steric effects are superimposed upon internal conjugate base rate enhancements for reactions involving Ni(II) ion with unprotonated ligands and that the magnitude of the ICB effect is a direct function of multidentate ligand basicity.

Other ligands such as N,N,N',N'-tetrakis(2-hydroxyethyl)ethylenediamine (TKED), N,N,N',N'-tetrakis(2-hydroxypropyl)ethylenediamine and amino acids (13,19,20) react anomalously slowly with Ni(II) ion. These results have been rationalized by assuming that the rate-determining step in the reaction mechanism is shifted to the loss of a second water molecule. In these reactions, "sterically controlled substitution" may occur when steric constraints block "normal substitution" (5) or when chelate ring closure is sufficiently slow as to become the rate-determining step.

Another widely studied type of complexation reaction involves multidentate ligand transfer between two metal ions, as represented by equation 9. These metal exchange reactions have been the subject of extensive study for a variety of metal ion combinations and aminocarboxylate ligands (21-31)

$$M + M'L \longrightarrow M' + ML \qquad (9)$$

The mechanism of these reactions has been shown to follow

the successive breaking of a series of coordinate bonds from the metal-ligand complex, followed by a stepwise coordination to the attacking metal (21-23,26-29,31). This process leads to the formation of a dinuclear intermediate found in all cases where sterically possible (23, 25,30) followed by breakup to form products. The stability of each reaction intermediate relative to the reactants can be estimated from the stability constant of the coordinated ligand segments to each metal and terms estimating electrostatic attraction or repulsion. Further, the rate constant for each step can be estimated from the exchange rate constant of the aquometal ion and the stability constant of the coordinated segment. Finally, a change in reactant concentration and hydrogen ion concentration can cause a shift in the rate determining step (28,31).

Polyaminocarboxylate ligands having N-alkyl-substituent branching have not been studied with respect to formation reactions. Steinhaus has recently investigated metal exchange reactions using ethylenediaminediacetic acid derivatives having alkyl substituents on the acetate arms (32,33). These studies have shown that an α-methyl group substituted on the acetate arms of EDDA resulted in a 10-fold decrease in the exchange rate of copper with ethylenediamine-N,N'-di-α-propionatonickel(II) (NiEDDP) and prevented a shift in reaction order with respect to copper as the copper concentration was varied (32). The related system involving 2,7-diisopropyl-3,6-diazaoctanedioatonickelate(II) and copper which has α-isopropyl groups substituted on the acetate arms of EDDA is currently understudy and appears to react in a fashion similiar to NiEDDP (33).

The present study was undertaken to investigate the mechanism of nickel complex formation with a sterically

hindered aminocarboxylate ligand, to establish the mechanism of the metal exchange reaction of this complex) with copper(II) and to determine the extent of the steric hinderance of a N-methyl group on a polyaminocarboxylate. The reactions chosen are shown in equations) 10 and 11, and involve Ni(II) with N,N'-dimethylethylenediaminediacetic acid, abbreviated DMEDDA (Structure I), which is shown here with protonation representative of the predominate reactant in neutral solution and copper(II) with N,N'-dimethylethylenediaminediacetatonickelate(II), abbreviated as NiDMEDDA

$$Ni^{2+} + HDMEDDA^{-} \longrightarrow NiDMEDDA + H^{+} \qquad (10)$$

$$NiDMEDDA + Cu^{2+} \longrightarrow CuDMEDDA + Ni^{2+} \qquad (11)$$

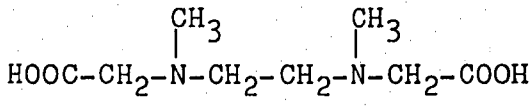

Structure I

The kinetic study of the rate of complex formation was designed so as to determine the location of the rate determining step. From previous studies, both ICB and steric effects were anticipated for this reaction.

The nickel complex formation study will attempt to show (i) that reaction 10 proceeds by the Eigen mechanism, (ii) the sequence of bond formation, (iii) the presence or absence of the ICB effect, and (iv) the magnitude of the steric effect. Comparison will be made of this study with other work on the kinetics of formation of Ni(II) complexes with a variety of ligands analogous to DMEDDA.

The kinetic study of the metal exchange reaction is

patterned after the work on copper(II) and ethylenediaminediacetonickelate(II) (31). From a consideration of the general mechanism for this type of a reaction and the similarity of the ligands, it was surprising that the present study found that the reaction proceeded by a copper independent pathway and that the observed rate constant is two order of magnitude smaller than for the similar system studied by Steinhaus and Swann (31).

EXPERIMENTAL

Chemicals

Reagent grade chemicals were used except as noted. All solutions were made using double distilled water and all stock solutions were filtered through a 0.45 micron Millipore filter at the time of preparation.

Double distilled water

Distilled water was passed through an ion exchange column containing a mixed bed resin (Amberlite MB-3) prior to its introduction to the first still. Two all glass stills were set-up in series and a polypropylene container was used to store the distillate.

Acetic acid-sodium acetate buffer

Sodium acetate ($NaC_2H_3O_2 \cdot 3H_2O$), from the J.T. Baker Co., (270 g) was dissolved along with 60 mL of glacial acetic acid and one liter of water to give a 3 M solution (acetate concentration) at pH 5.0.

Ammonia-ammonium chloride buffer

Ammonium chloride (NH_4Cl), from the J.T. Baker Co., (70 g) was dissolved in 430 mL of water to which 570 mL of concentrated ammonium hydroxide was added to produce a buffer with a pH value of 10.0.

HEPES Buffer

The buffer HEPES (N-2-hydroxyethylpiperzine-N'-2-

ethanesulfonic acid), pK_a 7.55 (34), was obtained from the Sigma Chemical Co. This buffer was used over the 6.8 to 8.2 pH range at a concentration of 0.05 M.

MES Buffer

The buffer MES (2[N-morpholino]ethane sulfonic acid), pK_a 6.15 (34), was obtained from the Sigma Chemical Co. This buffer was used over the 5.5 to 6.7 pH range at a concentration of 0.05 M.

TAPS Buffer

The buffer TAPS (tris[hydroxymethyl]methylamino-propane sulfonic acid), pK_a 8.4 (34), was obtained from the Sigma Chemical Co. This buffer was used over the 7.7 to 9.1 pH range at a concentration of 0.05 M.

CHES Buffer

The buffer CHES (cyclohexylaminoethane sulfonic acid), pK_a 9.55 (34), was obtained from the Sigma Chemical Co. This buffer was used over the 8.6 to 10.0 pH range at a concentration of 0.05 M.

Primary standard copper(II) nitrate

A standard solution of copper nitrate was prepared by weight from a heavy copper foil. This latter constituent at 99.96% purity was obtained from the J.T. Baker Co. The preparation entailed rinsing the foil with dilute nitric acid, deionized water, and absolute ethanol. The copper foil was then dried, weighed, and dissolved in a minimum amount of concentrated nitric acid. After

dilution to volume, the concentration was 0.09616 M.

Nickel(II) perchlorate

Nickel(II) perchlorate ($Ni(ClO_4)_2 \cdot 6H_2O$) was obtained from the G. Fredrick Smith Chemical Co. A solution was prepared and standardized at pH 10 (NH_3 - NH_4^+ buffer) and 60°C by titration with EDTA using murexide as an indicator.

Copper(II) perchlorate

Copper(II) perchlorate ($Cu(ClO_4)_2 \cdot 6H_2O$) was obtained from the G. Fredrick Smith Chemical Co. A solution was prepared and standardized at pH 10 (NH_3 - NH_4^+ buffer) by titration with EDTA using murexide as an indicator.

EDTA

Ethylenediaminetetraacetic acid, disodium salt dihydrate, was supplied by the Aldrich Chemical Co. The purity of this compound was in excess of 99% (Gold Label brand). Standardization of EDTA was performed by titration against a standard copper nitrate solution at pH 10 (NH_3 - NH_4^+ buffer), using murexide as an indicator.

Ionic strength

Sodium perchlorate ($NaClO_4$) was supplied by the J.T. Baker Co. A 5.0M solution was prepared by dissolving 306 grams of anhydrous sodium perchlorate in water and diluting to volume in a 500 mL volumetric flask. This stock solution was used to prepare all required ionic strength control solutions.

N,N'-dimethylethylenediaminediacetic acid

N,N'-dimethylethylenediaminediacetic acid was prepared by the reaction of 1,2 dibromoethane with sarcosine in the presence of a base (35).

$$2\ HN(CH_3)CH_2COO^- + BrCH_2CH_2Br \xrightarrow[H_2O\text{-}ETOH]{OH^-,\ CO_3^{2-}} CH_3N(CH_2COO^-)CH_2CH_2N(CH_2COO^-)CH_3 \quad (12)$$

Sarcosine (44.5 g, 0.5 mol), Columbia Organic Chemical Co., was dissolved in 100 mL of water containing sodium hydroxide (20 g, 0.5 mol). To this solution, 100 mL of water, 125 mL of 95% ethanol and 53.2 g (0.5 mol) of anhydrous sodium carbonate were added. The mixture was heated to reflux and a total of 47.0 g (0.25 mol) of 1,2 dibromoethane, Aldrich Chemical Co., was added over a period of six hours. Refluxing was continued for a further three hours after which the reaction was allowed to stand overnight. The ethanol was distilled from the mixture and the distillation continued until a white precipitate started to form in the reaction mixture.

The reaction mixture was allowed to cool to room temperature and 300 mL of 37% hydrochloric acid was added with cooling. The resultant white precipitate was filtered and washed with a minimum volume of cold 10% hydrochloric acid followed by a minimum volume of cold water. The precipitate was then dried at 60°C

The filtrates were combined and reduced in volume four more times, with each volume reduction resulting in the precipitation of white crystals. Each precipitate was treated as before and then was tested for the presence of DMEDDA by adding a small amount (~0.1 g) to 5 mL of a copper nitrate solution and adjusting the pH to 4 by

the dropwise addition of base. Only the last precipitate failed to give a strong positive indication (intense blue coloration) for the presence of DMEDDA. Therefore, the last precipitate was rejected along with all remaining filtrates.

The precipitates were combined (crude yield of 47 g (64%)) and dissolved in 50 mL of boiling water to which 10 mL of 37% hydrochloric acid had been added. The solution was filtered while hot and then reduced in volume until crystallization started. After cooling to room temperature the material was allowed to stand overnight. The precipitate was then removed by filtration, washed with a minimum volume of 10% hydrochloric acid, and suction dried. It was then was placed in a vacumm desiccator with sodium hydroxide pellets acting as a desiccant to neutralize any excess hydrochloric acid, dried at 60°C under reduced pressure for twenty four hours, and weighed.

The final yield was 29 g (39%) which melted at 226 - 229°C with decomposition. Spectrophotometeric titration of the DMEDDA with standard copper nitrate at 685 nm (pH 5.0, acetic acid-sodium acetate buffer) as shown in Figure 1, gave a purity of 88.3% calculated as DMEDDA·2HCl. A potentiometric titration, performed at 25°C under a nitrogen atmosphere using carbonate free sodium hydroxide gave a purity of 89.0% calculated as DMEDDA·2HCl with 20.9% chloride present in the form of hydrochloric acid. Analysis for total chloride (Mohr method) showed the sample to contain 27.8% total chloride. This discrepency between the two chloride determinations indicates an impurity level of 11.5%, calculated as sodium chloride. Elemental analysis was performed by Midwest Microlab LTD. Analysis for $C_2H_{18}N_2O_4Cl_2 \cdot xNaCl$, where x represents the percentage of sodium chloride present in the sample, gave

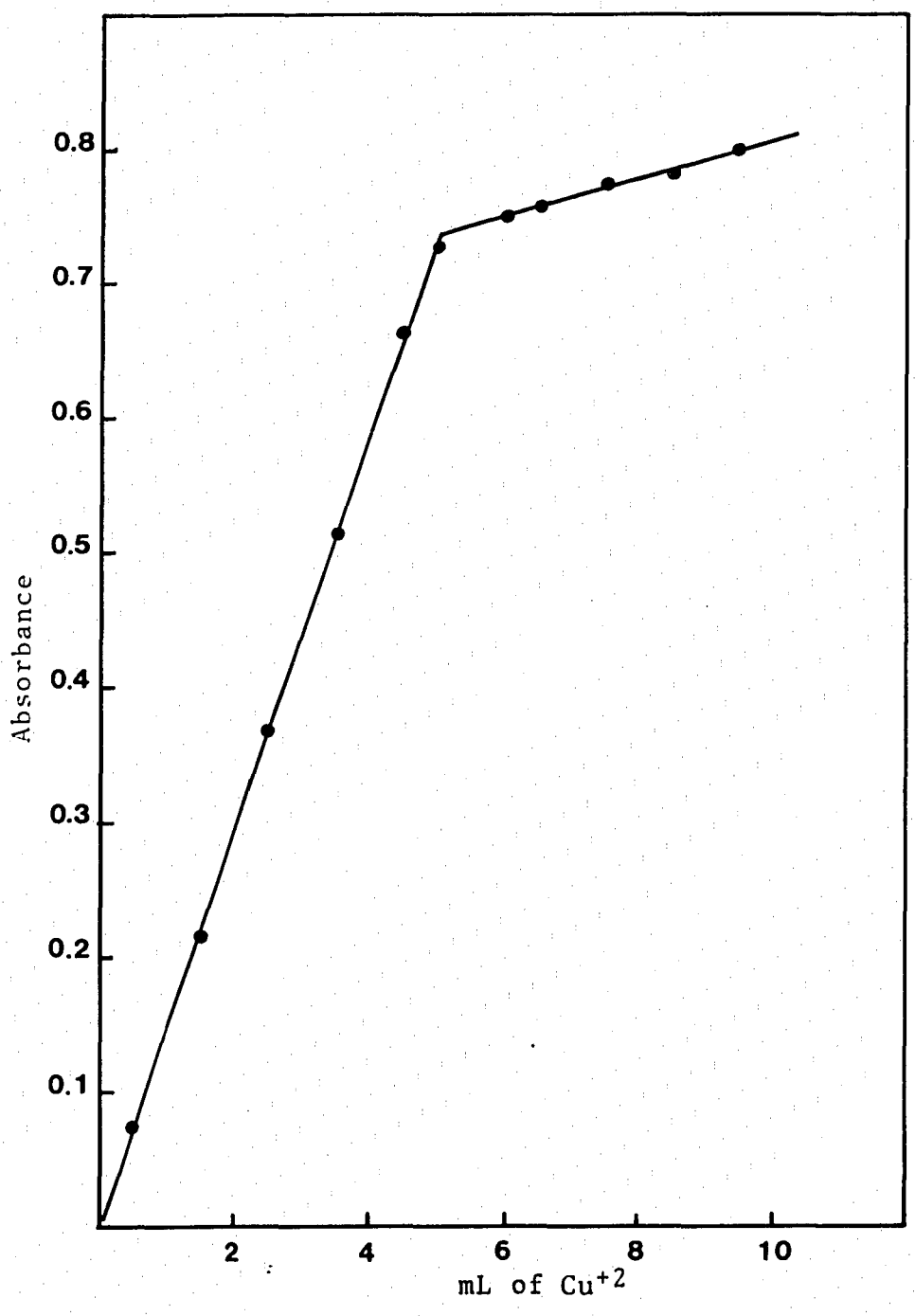

Figure 1. Spectrophotometric titration of DMEDDA at 685 nm and pH 5.0.

	%C	%H	%N	%O
Calculated	32.55	6.16	9.49	21.68
Found	33.68	6.74	9.73	22.39

Proton NMR spectroscopy performed at 60 MHz produced a NMR spectrum as shown in Figure 2 that was consistent with the structure of DMEDDA. Examination of the NMR baseline indicated that the material was free of contamination by sarcosine hydrochloride which would have resonated at 2.84 and 4.02 ppm(δ) with both resonances being a singlet (36).

Due to the presence of an impurity, the mole ratio method was used to standardize the DMEDDA with standard $Cu(NO_2)_2$ at a wavelength of 685 nm and pH 5.0 (acetic acid - sodium acetate buffer).

N,N'dimethylethylenediaminediacetatonickelate(II)

In order to prepare a NiDMEDDA solution, a slight molar excess (about 5%) of nickel(II) perchlorate solution was added to a standardized DMEDDA solution. The pH was adjusted to 11, to precipitate the excess nickel as the hydroxide. The solution was then filtered through a 0.45 micron Millipore filter, in order to remove the precipitate of nickel(II) hydroxide. The resulting solution was free of particulate and its pH was lowered to 8 by the addition of perchloric acid. A spectrophotometric method was employed to standardize the NiDMEDDA solution. The standardization involved determination of the nickel content at 267 nm. This was accomplished by adding a 100-fold excess of KCN (using an ammonia - ammonium chloride buffer system at pH 10) to the unknown to obtain $Ni(CN)_4$. The absorbance of this latter solution was then compared

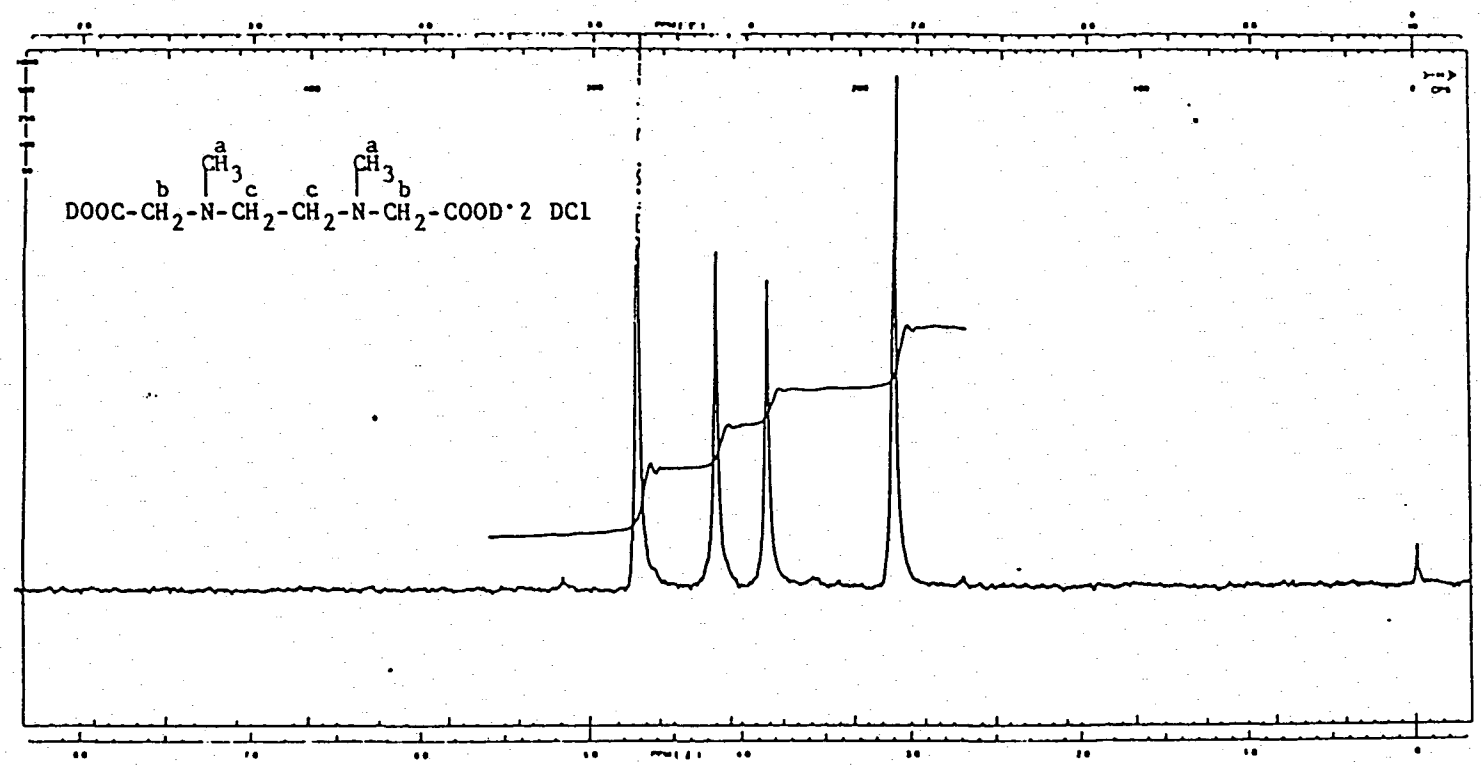

Filter bandwidth:	0.4	Hz		ASSIGNMENTS
Sweep time:	500	sec		
Sweep width:	500	Hz	a	3.11
Sweep offset:	-	Hz	b	3.86
Spectrum amp:	10		c	4.26
Intergal amp:	80		d	4.73 HDO
Solvent: D_2O				

Figure 2. NMR spectra of N,N'-dimethylethylenediaminediacetic acid, dihydrochloride

to the absorbance of a standard tetracyanonickelate(II) solution prepared from standard $Ni(ClO_4)_2$ and a 100-fold excess of KCN at pH 10.

Apparatus and Procedure

All spectra were recorded using a Cary Model 14 spectrophotometer. Kinetic measurements of formation reactions were made using an Aminco Morrow Stopped-Flow Apparatus attached to a Shimadzu QV-50 spectrophotometer. A Tektronic 5103N storage oscilloscope was employed to monitor the spectral changes. In addition, these spectral changes were stored on a Biomation Waveform Recorder (Model 805) and displayed from memory on a Model SR Sargent-Welch Recorder. Kinetic measurements for the rate of exchange were made using a Gilford 2000 Multiple Sample Absorbance Recorder in conjucntion with a Beckman DU Spectrophotometer.

A Beckman Research Model 1019 pH Meter, which possesses a relative accuracy of ±0.001 pH units, was employed for all pH measurements. All pH measurements were done at a temperature of 25.0±0.1°C.

The final pH for each solution used in the rate of formation study was obtained by measuring the pH of a solution produced by mixing equal volumes of each reactant. To prevent interference due to the formation of nickel(II) hydroxide, the pH of the nickel solutions were maintained at a pH of 5, and the pH of the ligand solutions were adjusted to a value slightly greater then desired. Several noncomplexing buffers were employed to maintain the desired pH.

The final pH for each solution in the rate of exchange study was obtained by measuring the pH of the reactant mixture prior to its introduction into the cell.

Prior to mixing of the reactants, the pH of each reactant was adjusted to the desired pH. Since there is no net change in the hydrogen ion concentration during the course of the reaction (see equation 11), all kinetic measurements were made with unbuffered solutions.

The wavelength of maximum absorbance for the formation studies was located by the following procedure. Absorption spectra of aqueous solutions of the ligand L and Ni(II) complex NiL were taken at known concentrations of their respective solutions. These spectra were taken in the ultraviolet spectral region in which the ligand L showed a moderately strong absorption. However, the absorption of the complex NiL was much greater. It was possible to find a wavelength at which there was a marked difference between the absorptions of the ligand L and the complex NiL. At 240 nm, the complex NiL and the free ligand L each possess an absorption. The molar absorptivities of the free ligand L and the complex NiL at this wavelength are 46 and 237 $L\text{-}mole^{-1}\text{-}cm^{-1}$ (see Table 1) respectively. Therefore, a wavelength of 240 nm was chosen to monitor the kinetics of the reactions between Ni(II) ion and the ligand L.

The rate of formation of the ligand complex was examined using a stopped-flow technique. Prior to each run, an appropriate buffer was added to the ligand solution to give a total buffer concentration of 0.05 M upon mixing with the nickel(II) solution. The ionic strength of each reactant solution was adjusted to 0.1 M with 1.0 M sodium perchlorate and the pH of the ligand solution was adjusted to the desired final pH by the addition of sodium hydroxide. The temperature was maintained at 25.0±0.1°C by the means of a constant temperature bath connected to the reservior site of a compartment within the stopped-flow apparatus. The wavelength

Table 1

Molar Absorptivities of DMEDDA and NiDMEDDA at 240 nm[a]

Speciecs	Concentration[b] (M)	Cell Length (cm)	Abs.[c]	Molar Absorptivity
DMEDDA	9.44×10^{-3}	1	0.431	45.7
	7.44×10^{-3}	1	0.348	46.1
	5.66×10^{-3}	1	0.262	46.3
	Average Molar Absorptivity: 46.0±0.3			
NiDMEDDA	4.88×10^{-4}	1	0.528	238
	3.01×10^{-4}	1	0.491	235
	2.15×10^{-4}	1	0.475	236
	1.03×10^{-4}	1	0.454	238
	Average Molar Absoptivity: 237±2			

a. Ionic strength, μ = 0.1M; pH = 8.0 (HEPES buffer at a total concentration of 0.05 M)

b. Refers to total concentration of ligand or complex

c. Referenced against a solution of 0.05 M HEPES buffer at pH 8.0 and a total ionic strength of 0.1 M

control of the Schimadzu QV-50 spectrophotometer was set at 240 nm, which gave a maximum absorbance change between product and reactant.

For each set of reaction conditions the formation of the complex NiL was followed by measurement of percent transmittance (%T) versus time (t). A preliminary run was performed in order to obtain a value for the final percent transmittance which could be read from the oscilloscope trace. On initiating a reaction, %T values versus time changes were stored in the Biomation Waveform Recorder as the reaction progressed. These values were subsequently displayed on a Sargent-Welch Model SR Recorder. From this latter trace, it was possible to make a table of %T versus time, which was then entered into a computer file so that calculations, for the purpose of extracting rate coefficients from the data, could be performed.

The kinetic measurements were made under pseudo-first-order conditions in which the total ligand was present in at least a 10-fold excess over that of the Ni(II) ion and the pH was systematically varied over the pH range of 6.0 - 9.5. Each reported kinetic run is for a specific set of reaction conditions and is the average of three to six separate stopped-flow runs.

The wavelength of maximum absorption for the exchange reaction was located by the following procedure. Absorption spectra of aqueous solutions of the NiDMEDDA complex and the CuDMEDDA complex were taken at known concentrations of their respective solutions. These spectra were taken in the visible region in which the NiDMEDDA complex showed a weak absorption. However, the absorption of the CuDMEDDA complex was much stronger. At 685 nm, the CuDMEDDA complex possesses its maximum absorbance with a molar absorptivity of 151 $L\text{-}mole^{-1}\text{-}cm^{-1}$ and the NiDMEDDA complex has a molar

absorptivity of 2.9 $L\text{-}mole^{-1}\text{-}cm^{-1}$ (see Table 2). The wavelength of 685 nm was chosen to monitor the exchange reaction.

The rate of exchange between NiL and Cu(II) ion was examined using a Gilford 2000 Multiple Sample Absorbance Recorder attached to a Beckman Model DU Spectrophotometer. Prior to each run, the ionic strength of the copper(II) solution was adjusted to 1.25 M by the use of 5.0 M sodium perchlorate and the pH of this solution was adjusted to the desired final pH by the addition of sodium hydroxide or perchloric acid. The temperature was maintained at 25.0±0.1°C by the means of a constant temperature bath connected to the cell compartment of the spectrophotometer. The wavelength control of the Beckman DU Spectrophotometer was set at 685 nm, which gave a maximum absorbance change between product and reactant.

For each set of reaction conditions the formation of the complex CuL was followed by measurement of absorbance (abs.) versus time t. From this trace it was possible to make a table of absorbance versus time, which was then entered into a computer file so that calculations, for the purpose of extracting rate coefficients from the data, could be performed.

The kinetic measurements for the rate of exchange were made under pseudo-first order conditions in which Cu(II) ion was present in a 10 to 50-fold excess over that of the NiDMEDDA complex. For all kinetic runs, the pH was held constant at a pH of 3.26.

Table 2

Molar Absorptivities of NiDMEDDA and CuDMEDDA at 685 nm[a]

Speciecs	Concentration (M)	Cell Length (cm)	Abs.	Molar Absorptivity
NiDMEDDA	1.01×10^{-3}	10	0.030	2.98
	2.21×10^{-3}	10	0.064	3.02
	4.07×10^{-3}	10	0.118	2.90
	5.93×10^{-3}	10	0.169	2.85
	Average Molar Absorptivity: 2.94±0.08			
CuDMEDDA	5.18×10^{-4}	2	0.153	149
	1.09×10^{-3}	2	0.332	152
	2.46×10^{-3}	2	0.726	148
	3.78×10^{-3}	2	1.163	154
	Average Molar Absorptivity: 151±3			

a. Ionic strength, μ = 1.25 M; pH = 5.0 (acetic acid-sodium acetate buffer)

RESULTS

Data Reduction

All formation reactions were carried out to completion; the exchange reactions were carried out through at least 2.5 half-lives. For all runs, pseudo-first-order conditions were maintained. The formation reactions were carried out by using at least a ten-fold excess (in total concentration) of ligand with respect to nickel(II) ion and the exchange reactions were carried out by using at least a ten-fold excess of copper(II) ion with respect to the NiDMEDDA concentration.

Initially the first-order rate expression shown in equation 13 was tested in both the formation and exchange

$$\frac{d[Ni] \text{ or } [NiL]}{dt} = k_o[Ni] \text{ or } [NiL] \qquad (13)$$

studies. Plots of the integrated form of equation 13 were linear for at least three half-lives thus establishing first-order behavior in nickel for the formation study and first-order behavior in NiL in the exchange study. Typical first-order plots are shown in Figure 3 for the formation study and Figure 4 for the exchange study. From this point on, an itterative curve fitting program was used to calculate the rate constants from the raw kinetic data. The method used involved a non-linear least squares analysis. The input data set for this program consisted of percent transmittance or absorbance values versus time for a completed kinetic run. The output consisted of three parameters and their corresponding standard deviations. Two of the output values, A_f and A_d, were absorbance values. The first of these, A_f represents the final absorbance value for the reaction;

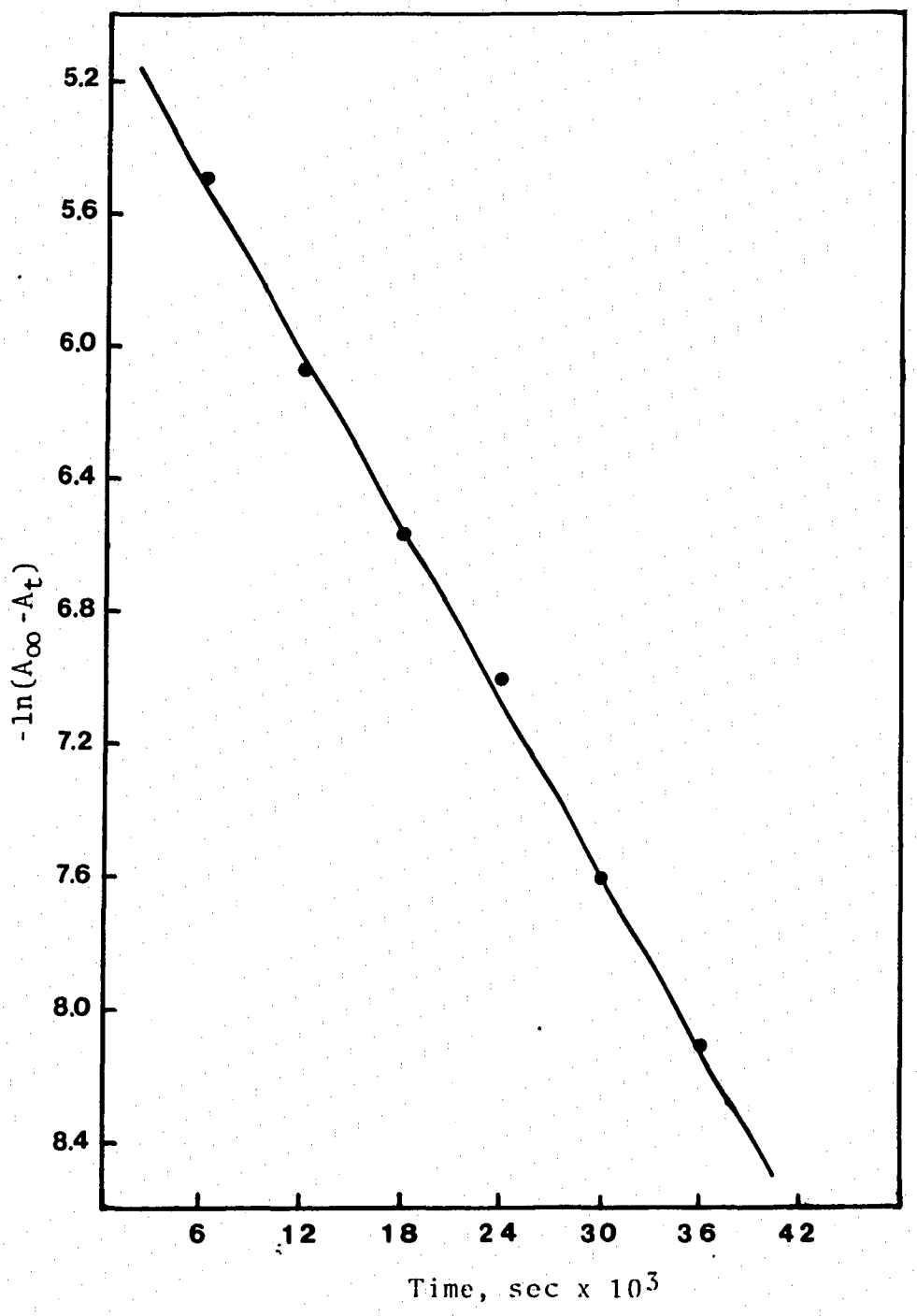

Figure 3. A typical first-order rate plot. Data for the rate of formation of NiDMEDDA.

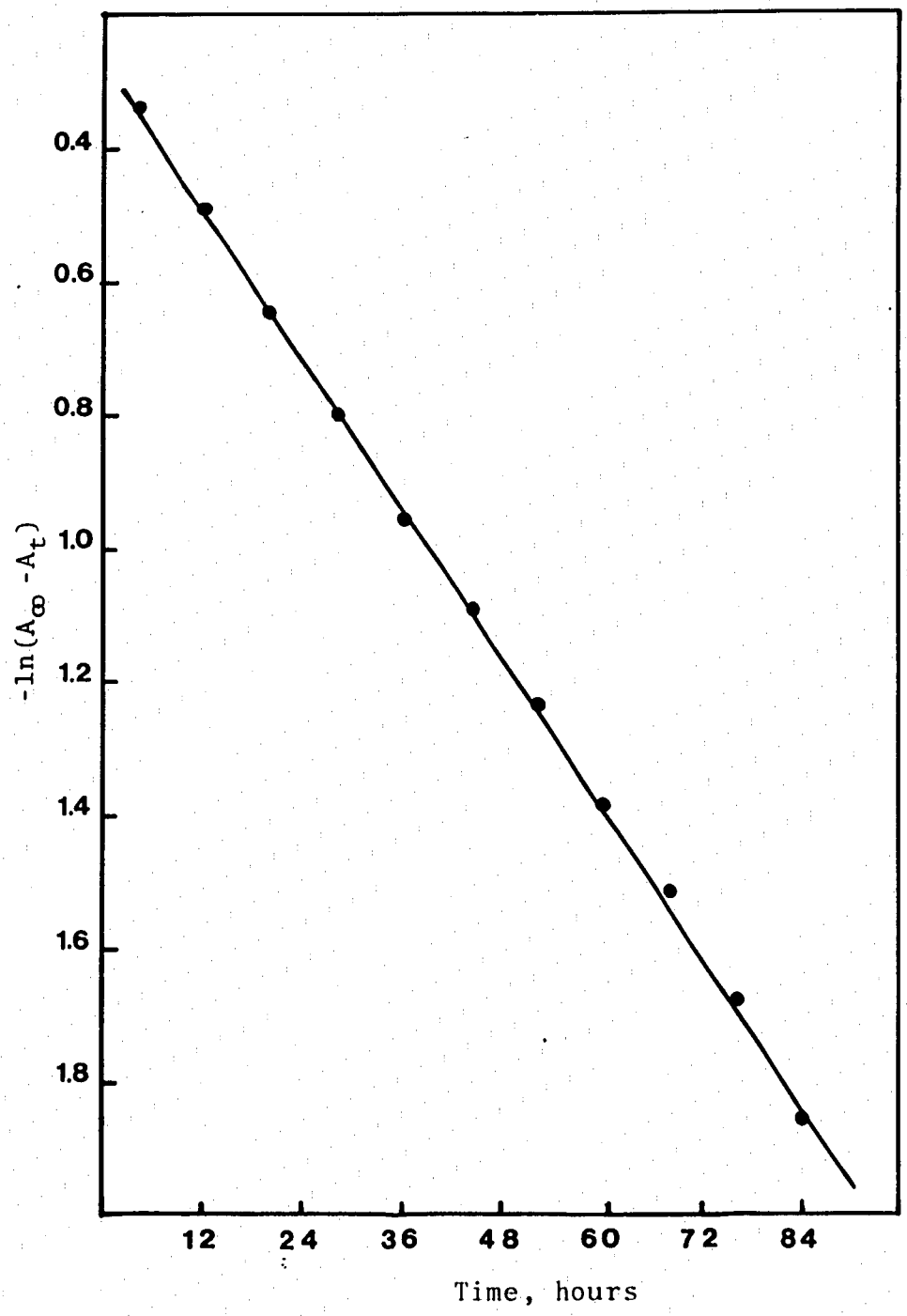

Figure 4. A typical first-order rate plot. Data for the rate of exchange between NiDMEDDA and Cu^{+2}.

this corresponds to time infinity. The latter, A_d, represents the absorbance change of the reaction mixture, denoted by $A_f - A_i$, where A_i is the initial absorbance of the reaction mixture. In the present study, product formation was followed, so that absorbance values always increased with reaction time t. The third and most important parameter obtained from the computer calculation was k_o, the pseudo-first-order rate constant. The formula in which all three of the above output variables are expressed is given by

$$A_t = (A_i - A_f)\exp(-k_o t) + A_f \qquad (14)$$

On the left-hand side of equation 14, the term A_t is the absorbance of the reaction mixture at time t. Rate constants for all kinetic runs were obtained by applying the above method.

Kinetic Systems Involving NiDMEDDA

Ni(II) - DMEDDA

The above system was studied over the pH range 5.9 to 9.3 using either HEPES, MES, TAPS, or CHES buffers at a concentration of 0.05 M. For this reaction a wavelength of 240 nm was chosen for study. The order in ligand was established by obtaining the pseudo-first-order rate constant, k_o, at various concentrations of total ligand at the same pH. Table 3 shows the kinetic data which are ordered in terms of increasing total ligand concentration. A plot of k_o versus total ligand concentration is shown in Figure 5 which demonstrates excellent linear behavior, thus establishing first-order behavior in total ligand. Since the reaction is first-order in

Table 3

Rate Constants k_o for the Reaction of DMEDDA with Ni(II)[a] at constant pH

$[L]_T \times 10^3$ M	k_o[b,c] s^{-1}	pH[d]
1.888	5.21	7.002
	5.26	
	5.13	
	ave. 5.20	
3.776	10.31	7.008
	10.40	
	10.48	
	ave. 10.40	
5.664	16.28	7.008
	16.60	
	17.22	
	ave. 17.70	
7.552	21.31	7.013
	21.56	
	21.72	
	ave. 21.53	
9.440	26.83	7.013
	27.24	
	28.57	
	ave. 27.55	
11.328	29.61	6.978
	33.05	
	34.70	
	ave. 32.45	

a. $[Ni^{2+}]_o = 1.801 \times 10^{-4}$ M

b. For all runs: T = 25.0±0.1° C, μ = 0.1 M

c. Reported as the average of the best of three out of five determinations.

d. HEPES buffer at a total buffer concentration of 0.05 M

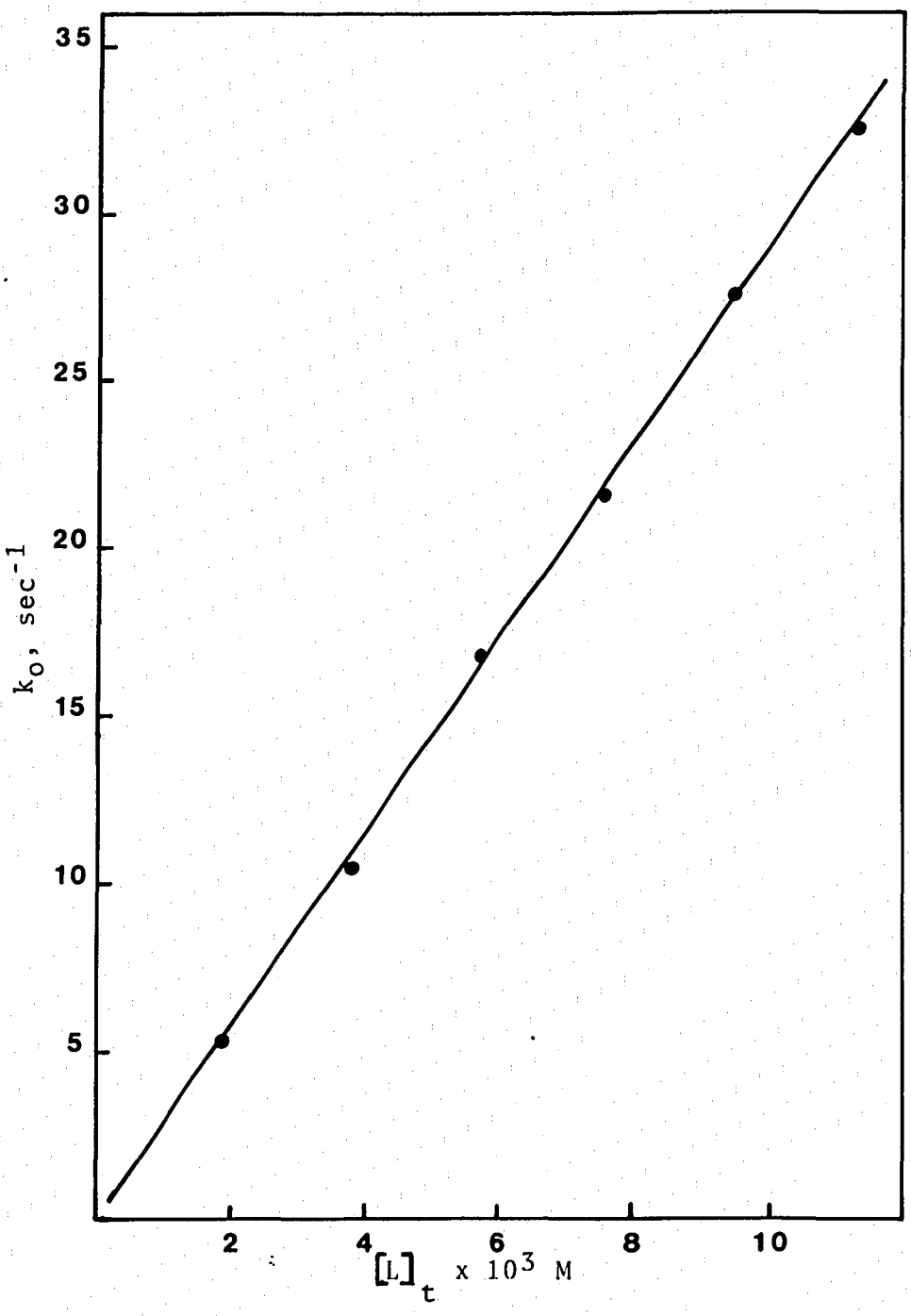

Figure 5. First-order rate plot for the formation of NiDMEDDA as a function of total ligand concentration.

nickel, the over-all reaction is second-order. All runs, as previously stated, were conducted at a total DMEDDA concentration $[DMEDDA]_T$ in excess over Ni(II) by a factor of at least ten.

Over the pH range studied, DMEDDA may exist in three distinct forms: $H_2DMEDDA$, $HDMEDDA^-$, and $DMEDDA^{2-}$. Since the dentate sites are blocked in the diprotonated species, this species is assumed to be unreactive. Consequently, for the Ni(II)-DMEDDA system, there are two simultaneous reactions leading to the formation of Ni(DMEDDA):

$$Ni(II) + DMEDDA^{2-} \xrightarrow{k_{Ni}^{L^{2-}}} Ni(DMEDDA) \qquad (15)$$

$$Ni(II) + HDMEDDA^{-} \xrightarrow{k_{Ni}^{HL^{-}}} Ni(DMEDDA) + H^+ \qquad (16)$$

Furthermore, the kinetic data can be resolved into the rate constants shown in reactions 15 and 16 according to the formula:

$$k_o = k_{Ni}^{HL^-}[HL^-] + k_{Ni}^{L^{2-}}[L^{2-}] \qquad (17)$$

The deprotonation of H_2L proceeds according to equations 18 and 19

$$H_2L \longrightarrow HL^- + H^+ \qquad (18)$$

$$HL^- \longrightarrow L^{2-} + H^+ \qquad (19)$$

with equilibrium constants (37) given by:

$$K_{a_1} = \frac{[HL^-][H^+]}{[H_2L]} = 1.03 \times 10^{-6} \qquad (20)$$

$$K_{a_2} = \frac{[L^{2-}][H^+]}{[HL^-]} = 1.06 \times 10^{-10} \qquad (21)$$

Solving equation 21 for $[L^{2-}]$ and substituting into equation 17 gives:

$$k_o = k_{Ni}^{HL^-}[HL^-] + k_{Ni}^{L^{2-}} K_{a_2} \frac{[HL^-]}{[H^+]} \qquad (22)$$

Equation 22 is easily rearranged to:

$$\frac{k_o}{[HL^-]} = k_{Ni}^{HL^-} + k_{Ni}^{L^{2-}} K_{a_2} \frac{1}{[H^+]} \qquad (23)$$

The concentration of HL^- can be determined using equation 24

$$[L]_T = [H_2L] + [HL^-] + [L^{2-}] \qquad (24)$$

which, after substituting appropriate values for $[H_2L]$ and $[L^{2-}]$ from equations 20 and 21, followed by a rearrangement gives equation 25. In equation 25, L_T refers to the total amount of ligand.

$$[HL^-] = \frac{L_T K_{a_1}[H^+]}{[H^+]^2 + K_{a_1}[H^+] + K_{a_1}K_{a_2}} \qquad (25)$$

In Table 4 are presented the kinetic data which are ordered in terms of increasing pH. Within this table are also presented concentrations of the reactive species, $HDMEDDA^-$ and $DMEDDA^{2-}$, and the pseudo-first-order rate constants k_o.

Figure 6 shows a plot of the left-hand side of

Table 4

Experimental Conditions and Rate Constants for the Reaction of Ni(II)[a] Ion with DMEDDA[b]

pH	$[L^{-2}] \times 10^5$ M	$[HL^{-}] \times 10^3$ M	k_o s^{-1}
5.998	0.02	1.91	5.79
6.098	0.03	2.13	6.22
6.405	0.07	2.73	8.60
6.699	0.17	3.16	8.63
7.110	0.48	3.64	12.8
7.252	0.68	3.75	13.4
7.400	0.97	3.63	15.7
7.620	1.62	3.67	19.6
7.808	2.52	3.69	18.5
7.901	3.12	3.70	24.2
8.058	4.48	3.70	22.8
8.223	6.53	3.69	25.3
8.516	12.7	3.64	27.7
8.776	22.4	3.55	40.9
9.018	37.5	3.40	56.2
9.140	48.1	3.29	79.5
9.220	56.4	3.21	94.2
9.334	70.2	3.07	117.1

a. $[Ni^{2+}]_T = 1.8 \times 10^{-4}$ M

b. $[DMEDDA]_T = 3.78 \times 10^{-3}$ M

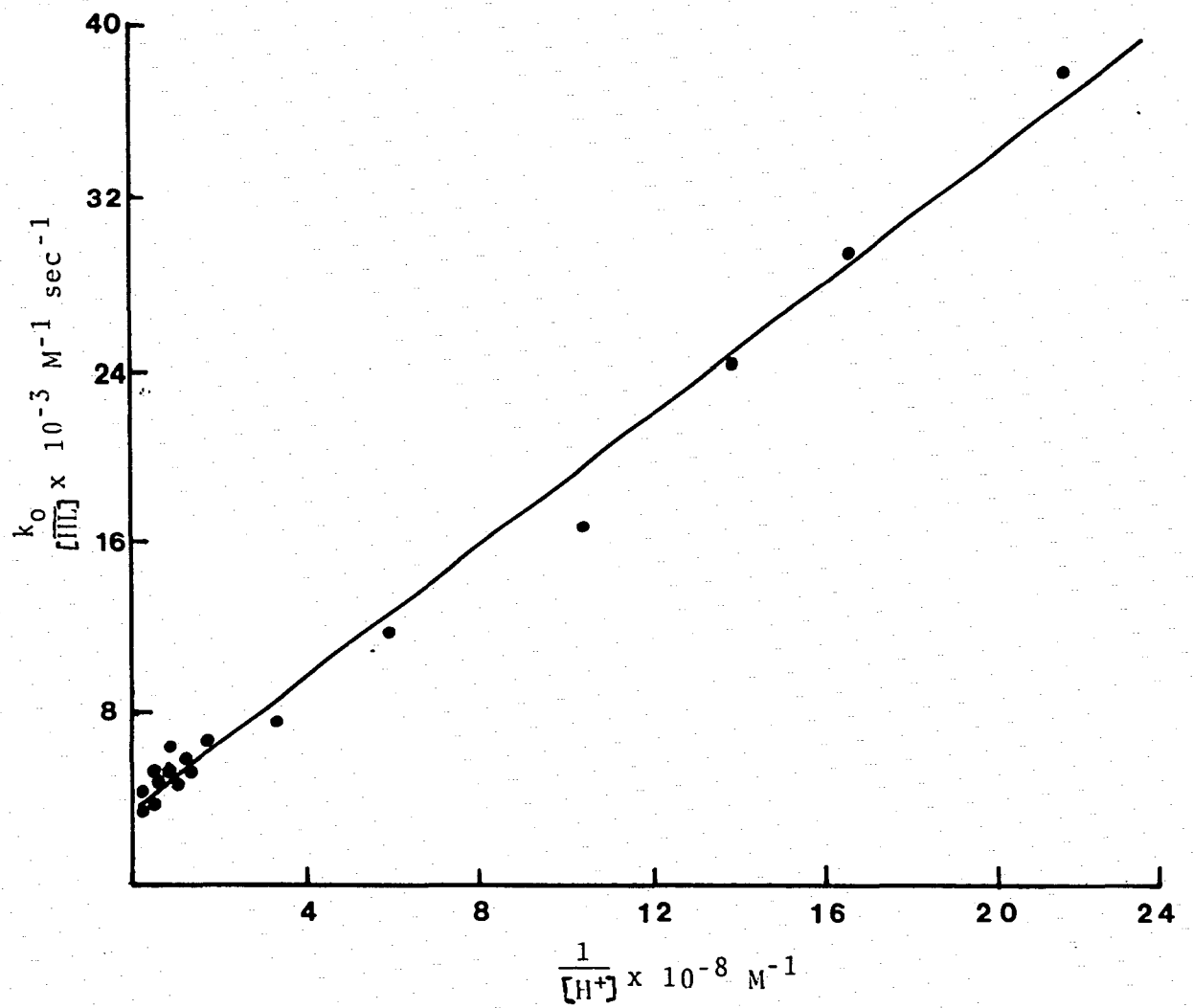

Figure 6. Resolution of rate constants k_{Ni}^{L} and k_{Ni}^{HL} for the formation of NiDMEDDA.

equation 23 versus the reciprocal of the hydrogen ion concentration using the data listed in Table 4. The line represents the least-squares best fit of the data. The slope and intercept correspond to the following terms in equation 23:

a) $k_{Ni}^{L^{2-}} K_{a_2}$, slope

b) $k_{Ni}^{HL^-}$, intercept

Rate constants for the reaction of both $HDMEDDA^-$ and $DMEDDA^{2-}$ are given in Table 5. Also reported within this table are the standard deviations for each rate constant along with the correlation coefficient for the kinetic plot. As Figure 6 shows, excellent linearity is obtained using equation 17 and therefore the assumption that the diprotonated species is unreactive is valid.

For DMEDDA, equation 22 allows calculation of the observed rate constant as a function of pH since the resolved rate constants, as given in Table 5, and the appropriate ligand concentrations are known. The calculated and experimentally determined values are presented in Table 6. Comparison of these calculated values with the experimentally observed values gives excellent agreement for the entire pH range studied. This is shown in Figure 7 in which the fraction of DMEDDA and the experimentally determined pesudo-first-order rate constant, k_o, are ploted as a function of pH. The solid curve for k_o represents the calculated values for k_o as a function of pH.

NiDMEDDA - CuDMEDDA Reaction

All kinetic runs for the NiDMEDDA-CuDMEDDA reaction were preformed at a wavelength of 685 nm on unbuffered

Table 5

Resolved Fromation Rate Constants for the Reaction of Ni(II) Ion with DMEDDA

Species	k_f $M^{-1}sec^{-1}$	Std. Dev. $M^{-1}sec^{-1}$
$H_2DMEDDA$	-0-	---------
$HDMEDDA^-$	3.50×10^3	6.9×10^2
$DMEDDA^{2-}$	1.46×10^5	8.4×10^3

Correlation Coefficient = 0.994

Table 6

Experimental and Calculated Values of the Observed Rate Constants as a Function of pH

pH	Calculated k_o, sec^{-1}	Experimental[a] k_o, sec^{-1}
5.998	6.71	5.79
6.098	7.50	6.22
6.405	9.66	8.60
6.699	11.3	8.63
7.110	13.4	12.8
7.252	14.1	13.4
7.400	14.4	15.7
7.620	15.2	19.6
7.808	16.6	18.5
7.901	17.5	24.2
8.058	19.5	22.8
8.223	22.5	25.3
8.516	31.2	27.7
8.776	45.2	40.9
9.018	66.7	56.2
9.140	81.8	79.5
9.220	93.6	94.2
9.334	113.3	117.1

a. For all runs: $T = 25.0 \pm 0.1°$ c, $\mu = 0.1M$

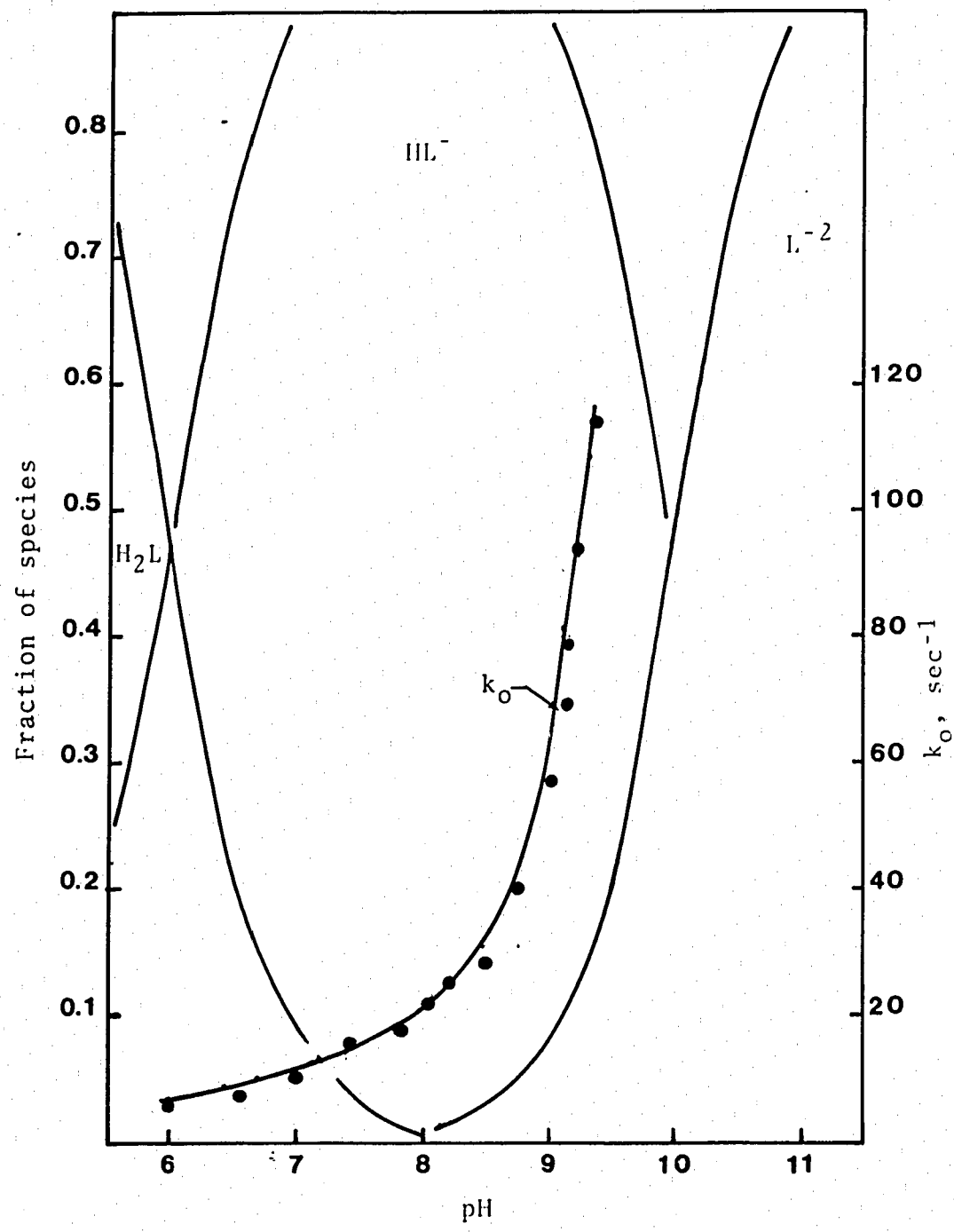

Figure 7. Fraction of DMEDDA and k_o as a function of pH

solutions which had been adjusted to a pH of 3.26 at an ionic strength of 1.25 M. The experimental results are provided in Table 7 where the pseudo-first-order rate constants are arranged according to increasing concentration of Cu(II) ion.

Table 7

Experimental Conditions and Observed Rate Constants for the Exchange Reaction Between NiDMEDDA[a] and Cu(II)

$[Cu^{2+}] \times 10^2$ M	$k_o^b \times 10^5$ sec^{-1}
0.532	5.58
0.822	4.63
1.336	5.23
1.542	5.43
1.850	6.15
2.055	5.53

a. $[NiDMEDDA]_T = 4.76 \times 10^{-4}$ M

b. For all runs: T = 25.0±0.1° C, μ = 1.25 M, pH = 3.26

Figure 8 shows a plot of the pseudo-first-order rate constant, k_o, versus the copper(II) concentration for a given pH. As Figure 8 demonstrates, the copper(II) dependence is zero-order. The reaction had previously been shown to be first-order in NiDMEDDA. Due to the extremely long half lives, approximately 39 hours, and the zero-order copper dependence, further investigation of this reaction was terminated.

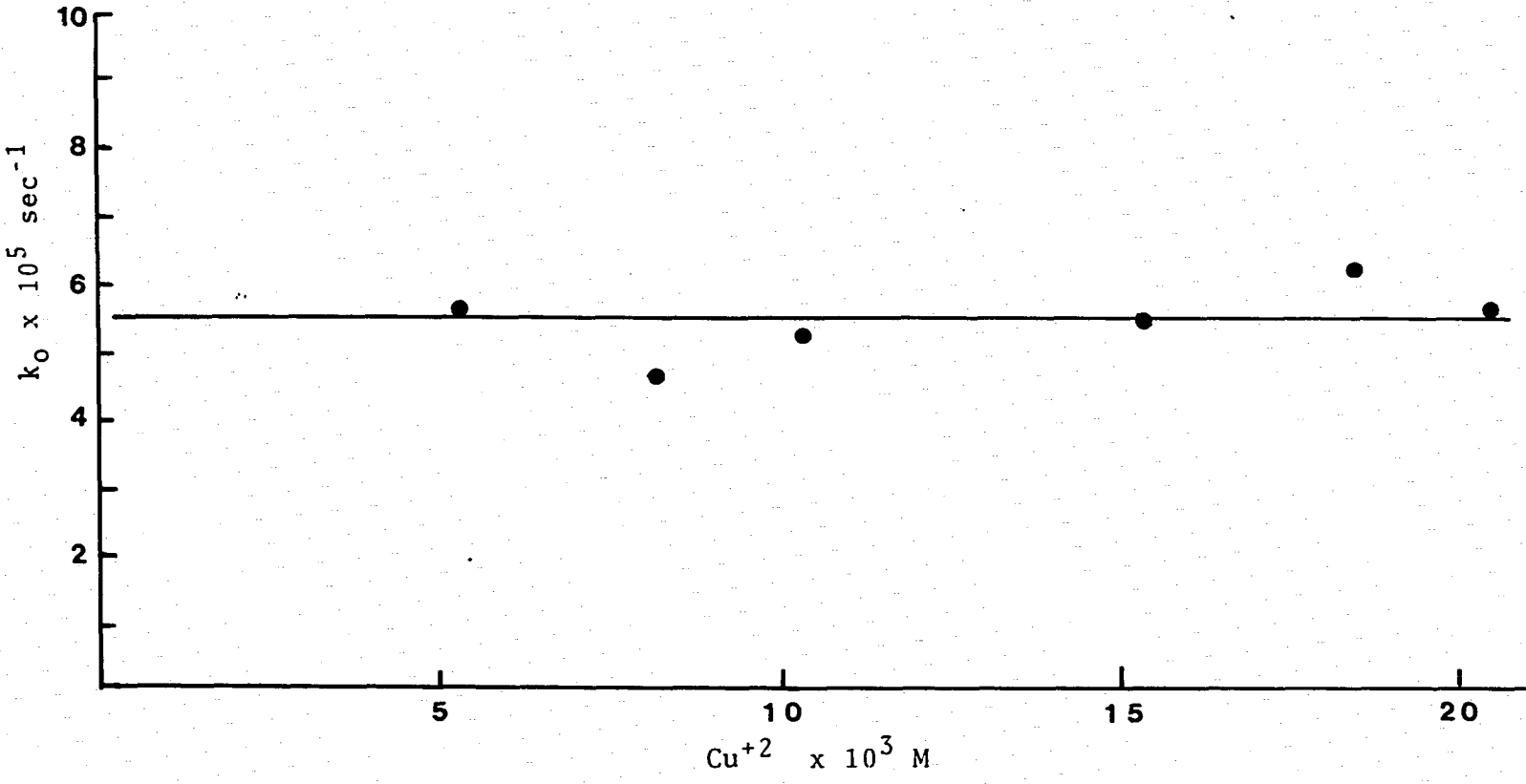

Figure 8. Observed exchange rate constant as a function of copper concentration at pH 3.26.

DISCUSSION

As stated in the Introduction, the Eigen-Tamm equations 7 and 8 are useful in predicting formation rates only for idealized systems, for these equations fail to take into consideration the effects that the ligand exert on the rate of formation. Experimental evidence has been advanced to show that modifications of the Eigen-Tamm mechanism are necessary. The most important factors that have better defined the nature of complex formation reactions, and are relevant to the present study include:

1) ICB (internal conjugate base) effects
2) Steric hindrance effects

Each of the above effects are dependent upon the nature of the ligand. In the system under study, the ICB effect is precluded for $HDMEDDA^-$, but must contribute to the reaction involving $DMEDDA^{-2}$, since this species contains a donor atom with a pK_a which is greater than eight. This high pK_a will allow the donor atom to form a hydrogen bond with a water molecule coordinated to the nickel(II) ion, thereby stablizing the outer-sphere intermediate and labilizing subsquent water loss. As a result, the ligand promotes its own coordination. ICB effects will be discussed in more detail in later sections. The second effect presented above involves steric hindrance and its mechanistic consequences and is focal point of the present study. It will be discussed in detail in the following sections.

General Mechanism for Nickel-DMEDDA Formation Reaction

On the basis of earlier studies (5,16) of nickel(II)-polyamine reactions, the nickel(II)-polyaminocarboxylate

reactions are presumed to follow a stepwise bonding of the ligand to the metal with the individual bonding steps being dissociative in nature (4). On this basis, the loss of a coordinated water molecule must precede the formation of each metal-donor bond and the short-lived nature of the five coordinate intermediate dictates that the reactants must be adjacent at the time of metal-water bond rupture in order for reaction to occur. Thus, the rate of initial bond formation is limited by the extent of ion-pair (outer-sphere) formation.

For DMEDDA, the rate-limiting step can occur no further in the mechanism sequence than coordination of the second dentate site or ring closure of the first ring. The reason is that closure of this ring coordinates an aliphatic nitrogen to nickel which, in turn, causes a 10-fold acceleration in the formation rate of the next dentate site (38). Since the rotational barriers for each ring are similiar, having only slight differences, which could not offset a 10-fold increase in the rate of water loss, the subsequent ring closure rates will be at least 10 times faster than the initial one.

The first dentate site to coordinate is the carboxyate group which is consistent with published results (39). There are several reasons why this weaker donor group is the first to bond: (1) electrostatic attraction, (2) ICB contribution from the stronger donor, and (3) secondary or tertiary nitrogen atoms.

Following the manner of Wilkins (5),the reaction mechanism is represented schematically in Figure 9. Assuming that (1) outer-sphere complex formation and dissociation rates are much faster than the subsequent steps, (2) the protonation equilibrium in the doubly bonded complex (K_H') is rapidly established relative to the rate of nickel-nitrogen bond rupture (k_{-2}'), (3) the

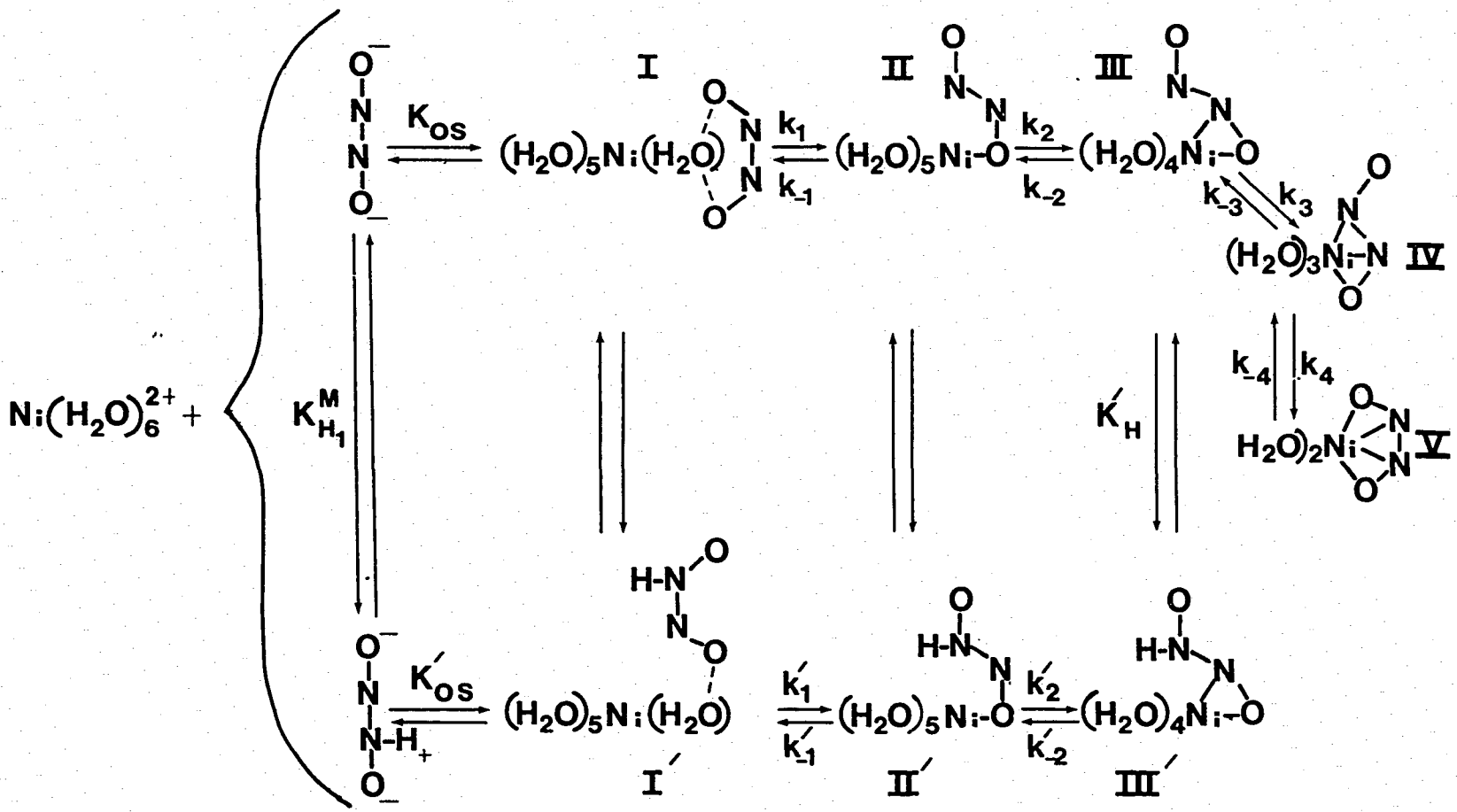

Figure 9. Schematic representation of the reaction mechanism for aquonickel(II) ion reacting with a tetradentate ligand. The diprotonated species is presumed to be unreactive.

steady-state conditions may be applied for the intermediates, and (4) the rate-determining step does not lie past step II→III, the rate constants in equation 17 may be related to the stepwise rate constants as

$$k_{Ni}^{L^{-2}} = \frac{k_2 k_1 K_{os}}{(k_{-1} + k_2)} = k_f \qquad (26)$$

$$k_{Ni}^{HL^-} = \frac{k_2' k_1' K_{os}'}{(k_{-1}' + k_2')} = k_f' \qquad (27)$$

Recognizing that any difference in the rate of formation between HL^- and L^{-2} would manifest itself in the values of K_{os} and K_{os}', and not in the rate constants for the individual steps, allows the prime designation for these steps to be droppped from equation 27.

Predicted Formation Rate Constants

In order to predict the formation rate constant, it will initially be assumed that chelate ring closure is much faster than breaking of the single bond in intermediate II so that $k_2 >> k_{-1}$, and the k_f value reduces to that in equation 28

$$k_f = K_{os} k_1 = K_{os} k^{Ni-H_2O} \qquad (28)$$

Actually, equation 28 can be used even when the rate constant for ring closure is nearly equal to the rate constant for breaking of the single bond in intermediate II. In this case,

$$k_f = \frac{1}{2} K_{os} k^{Ni-H_2O} \qquad (29)$$

and the predicated rate constant may be within experimental error of the observed rate constant.

It is necessary to evaluate both K_{os} and k^{Ni-H_2O}. The association constant, K_{os}, for the outer-sphere complex is estimated from diffusion theory using statistical considerations (7,8). The proposed equation for K_{os} is written:

$$K_{os} = (4/3)\pi Na^3 \times 10^{-3} \exp(-U_a/kT) \qquad (30)$$

In the above formula:

1) k is Boltzman's constant
2) T is Temperature (°K)
3) N is Avogadro's number
4) a represents the center-to-center distance between the ligand and Nickel(II) ion
5) U_a is the Debye-Huckel interionic potential given by

$$U_a = \frac{Z_M Z_L e^2}{a'D} - \frac{Z_M Z_L e^2 \kappa}{D(1+\kappa a')} \qquad (31)$$

In equation 31,

6) Z_M and Z_L are the formal charges on each of the reacting species M and L (metal and ligand respectively)
7) e represents the electronic charge
8) D is the dielectric constant of the solvent (D=78.59 for H_2O)
9) a' = center-to-center replusive distance between M and L
10) κ is the Debye-Huckel ion atmosphere parameter given by

$$\kappa^2 = \frac{8\pi Ne^2\mu}{1000DkT} \qquad (32)$$

and in equation 32,

11) N, e, D, k, and T are defined as before

12) μ = ionic strength

The value of a' was assigned using the following considerations: (1) the zwitterion is the major monoprotonated form of aliphatic amino acids, and (2) the dipolar end will behave as if it were a neutral species. Therefore, a reference state was chosen in that there is no net contribution from these charge centers in determining the theoretical value of K'_{os}. The unprotonated carboxylate group, which also bonds first, can be shown to be $4x10^{-8}$ cm from $Ni(H_2O)_6^{2+}$ using molecular models. Thus, $a = a' = 4x10^{-8}$ cm (with $Z_M = +2$ and $Z_L = -1$) and equation 30 gives $K'_{os} = 2\ M^{-1}$.

For the unprotonated species, a reference model was chosen in which both negatively charged acetate arms are electrostatically attracted to the positively charged nickel(II) ion with both center-to-center distances being equal. Using $a = a' = 4x10^{-8}$ cm with $Z_M = +2$ and $Z_L = -2$ in equation 30 gives $K_{os} = 20\ M^{-1}$.

According to equation 28, the formation rate constant, k_f, can be calculated using the above derived values of K_{os} and the literature value of k^{Ni-H_2O} ($2.7 \times 10^4\ s^{-1}$ (40)). A summary of all predicted and measured formation rate constants are presented in Table 8.

Reaction Of Nickel(II) With $HDMEDDA^-$

The experimental value for the formation rate constant, k_f, is lower by a factor of 15 (see Table 8). Thus, equation 28 does not apply and equation 27, which has ring closure as the rate-limiting step, must be used. Although no values have been directly measured for the dissociation rate constant k_{-1} of equation 27, it can

Table 8

Summary of Predicted and Experimental Formation Rate Constants

Species	K_{os} M^{-1}	Predicted k_f $M^{-1}\ s^{-1}$	Experimental k_f $M^{-1}\ s^{-1}$
$HDMEDDA^-$	2	5.4×10^4	3.50×10^3
$DMEDDA^{2-}$	20	5.4×10^5	1.46×10^5

be approximated by the known value (41) for pentaaquonickel acetate ($k_{-1} = 5 \times 10^3\ s^{-1}$). The value of k_1 remains equal to k^{Ni-H_2O}. Application of these values in equation 33

$$k_2 = \frac{k_f k_{-1}}{(K'_{os} k_1 - k_f)} = \frac{(3.5\times10^3 M^{-1}s^{-1})(5\times10^4 s^{-1})}{(2\ M^{-1})(2.7\times10^4 s^{-1}) - 3.5\times10^3 M^{-1}s^{-1}} \quad (33)$$

produces a value of 347 s^{-1} for the rate of ring closure, k_2. Thus $k_{-1} >> k_2$ and ring closure is rate limiting. The value of k_2 is a composite which consists of the rate of water loss from the nickel(II) ion and the energy barrier imposed by the necessity to twist the polyaminocarboxylate ligand into a configuration favorable for the second bond formation. This rotational barrier can be calculated by

$$r = \frac{k^{Ni-H_2O}}{k_2} \quad (34)$$

The energy barrier due to the twisting of the polyaminocarboxylate is estimated to be: $2.7 \times 10^4 / 347 = 78$ which through the application of equation 35

$$\text{Potential Barrier} = RT \ln r \qquad (35)$$

is equilvalent to a potential barrier of 2.6 kcal. $mole^{-1}$.

The energy barrier for rotation of a polyamine segment of trien has been esimated to be 44 (16) and that of a 2-hydroxy ethylamine group in TKED to be 30 (13). Thus, the value of 78 obtained in the present study is quite reasonable and represents a modest increase due to the N-methyl group present in DMEDDA.

Reaction Of $DMEDDA^{2-}$ With Nickel(II)

Since the reaction of $HDMEDDA^-$ proceeds with ring closure as the rate-limiting step and since $DMEDDA^{2-}$ is identical to $HDMEDDA^-$ save for the absence of a proton on the third dentate site to bond, it follows that ring closure must also be rate-limiting for $DMEDDA^{2-}$ and equation 26 expresses the appropriate terms in the formation mechanism.

Table 8 shows $DMEDDA^{2-}$ to react faster with $Ni(H_2O)_6^{2+}$ by a factor of 42 compared to $HDMEDDA^-$. This rate enhancement is attributed to a two fold effect. The larger formal charge on $DMEDDA^{2-}$ causes an increased electrostatic attraction to the positively charged nickel and results in a K_{os} value of 20 M^{-1} as compared to 2 M^{-1} which was found for the reaction involving $HDMEDDA^{-1}$. Also, the rate of formation is enhanced by the ICB effect. The ICB mechanism can be broken down into five steps: (1) the formation of an outer-sphere complex, (2) the establishment of a hydrogen bond between a coordinated water

other similar systems is hindered since some systems have not yet been studied and since an accurate value of the ICB effect for aminocarboxylate ligands has not been calculated. Comparision to EDDA, identical with DMEDDA except lacking the N-methyl groups, can not be made because the rate of formation of nickel EDDA complex has not been studied. Sarcosine is somewhat like DMEDDA in that it has an N-methyl group although it is a considerably smaller molecule. An indirect estimate for the ICB effect present as sarcosine reacts with $Ni(H_2O)_6^{2+}$ can be obtained from the recent study of the reaction of sarcosine and NiEDDA (42). A value of 8 was estimated in that study. The present study involves six open coordination sites whereas NiEDDA has only two. Thus statistically, the ICB value of 8 for NiEDDA and sarcosine should be multiplied by three to correct for the increased availability of sites on $Ni(H_2O)_6^{2+}$. Using an ICB effect of 24 along with other previously described term in equation 28, gives a value of $k_{Ni}^{sar} = 1.3 \times 10^6\ M^{-1}s^{-1}$, which is about 100 times greater than the experimental value of $1.3 \times 10^4\ M^{-1}s^{-1}$ (43). Thus as has been suggested (39), ring closure must be rate-limiting and equation 26 can be used to calculate the ring closure rate constant, k_2. Supporting evidence for rate-limiting ring closure of aminocarboxylates includes comparision of their rate of formation with that of polyamines (39). Equation 26 yields a value of 52 for ring closure of sarcosine on nickel. Similar calculations for the reaction of glycine with nickel, using an estimate of the ICB effect for the reaction of glycine with NiEDDA (a value of 32 is obtained (42)) yields a value of 130 for ring closure. Table 9 lists the results. Clearly, unhindered glycine has a larger value for k_2 compared to sarcosine. However, both gly and sar show k_2 values considerably less than

molecule and a basic donor atom of the ligand , (3) loss of a labilized water molecule from the inner sphere with rapid substitution of a second donor atom from the same multidentate ligand molecule, (4) rupture of the original hydrogen bond and (5) further bonding of the multidentate ligand by the normal reaction path as outlined in Figure 9. Modification of equation 26 by including a term for the ICB effect gives

$$k_f = k_{Ni}^{L^{-2}} = \frac{k_2 k_1 K_{os} k_{ICB}}{(k_{-1} + k_2)} \qquad (36)$$

Rearrangement of equation 36, followed by insertion of the values given earlier for k_{-1}, k^{Ni-H_2O}, K_{os}, k_2 and the experimentally determined formation rate constant k_f into equation 37

$$k_{ICB} = \frac{k_f(k_{-1} + k_2)}{(K_{os} k_1 k_2)} = \frac{1.46 \times 10^5 M^{-1}s^{-1}(5 \times 10^3 s^{-1} + 347 s^{-1})}{(20 M^{-1})(2.7 \times 10^4 s^{-1})(347 s^{-1})} \qquad (37)$$

gives a value of 4.2 for the ICB effect. This modest value for the ICB rate enhancement is a factor of 30 lower than an estimated value of 120 for the reaction of $DMEDDA^{2-}$ with nickel(II) ion. This estimate is based on the work of Turan (18) in which the internal conjugate base rate enhancement was shown to be a function of the ligand basicity. The graphical proof of this correlation (a plot of log ICB versus log K_{H1} where K_{H1} is defined as the protonation constant for the basic site) was used to estimate the internal conjugate base effect for $DMEDDA^{2-}$.

Comparision To Other Aminocarboxylate Systems

Comparision of the results from the present study to

Table 9

Comparision of the Rate of Ring Closure and ICB Effect for Sarcosine, Glycine, and DMEDDA

Species	Rate of Ring Closure sec^{-1}	ICB Effect	pK_a
Sarcosine	52	24	9.99
Glycine	130	32	9.57
DMEDDA	347	4.2	9.97

that of DMEDDA, which is a larger molecule with four dentate sites and which has negative charges on each of the terminal dentate sites. This has the effect of bringing the whole molecule of DMEDDA in close proximity to that of nickel such that very little rearrangment and rotation prior to ring closure is needed. Hence, a larger ring closure rate constant is expected. It is likely that comparision of ring closure rates between small bidentate ligands and large multidentate ligands is not valid. The steric effect of the N-methyl group can not be accurately determined until the formation reaction between $Ni(H_2O)_6^{2+}$ and EDDA is studied.

The ICB values for sar and gly, estimated to be 24 and 32 respectively, are higher then that of 4.2 found for DMEDDA. Although sar has an N-methyl group like DMEDDA, the nitrogens in DMEDDA are tertiary while that in sar is a secondary and the nitrogen of gly is primary.

Clearly larger ICB effects are to be expected from uncluttered, unhindered dentate sites and the values in the three cases cited above follow that pattern. The N-methyl group of DMEDDA does appear to limit the effectiveness of that ligand from participating in a strong ICB interaction. The pK_a values of sar and DMEDDA are almost indentical (9.99 and 9.97 respectively (37)) such that dentate site basicity does not cause any difference to be expected in these two ICB values. The pK_a of gly, 9.57 (37), is lower than sar and DMEDDA. Thus, the larger ICB effect seen for gly is deceiving and placed on a scale of basicity equal to that of sar and DMEDDA, the ICB effect of gly would be considerably larger. Thus secondary and tertiary nitrogens do limit the effectiveness of ICB participation.

NiDMEDDA-Copper(II) Exchange Reaction

The previous discussion has established that the rate-limiting step in the formation of NiDMEDDA from $Ni(H_2O)_6^{2+}$ and $DMEDDA^{2-}$ is the formation of the second bond. Microscopic reversibility thus dictates that the rate-limiting step in the dissociation of NiDMEDDA is rupture of the second nickel-nitrogen bond or opening of the third chelate ring of NiDMEDDA.

As shown in Figure 8 the copper(II) dependence is zero-order for the exchange reaction between NiDMEDDA and copper(II). For this to occur, the rate-determining step must occur prior to attack by copper(II) ion. After the rate-limiting step, copper may attack to form a dinuclear intermediate having the remaining carboxyl group of DMEDDA still bonded to nickel and one, two, or all three of the unwrapped dentate sites bonded to copper, or, DMEDDA may completely dissociate from nickel before forming a complex

with copper. In either case, the copper dependence is zero. The unusual feature of this zero order dependence is the inablity of copper to coordinate to the half-unwrapped DMEDDA or sarcosine segment. A possible explaination lies in the inablity of DMEDDA to unwrap from nickel and twist into a configuration suitable for bonding to copper before the rate-limiting step - rupture of the last nickel-nitrogen bond. It is evident from a consideration of molecular models that the N-methyl groups hinders rotation of the unchelated segments of DMEDDA thus making it difficult for copper to coordinate to the partially unwrapped ligand. This may prevent formation of a dinuclear intermediate prior to the rate-limiting step, a feature seen in metal exchange studies, and results in a zero-order behavior in copper. EDDA (31), having no such methyl substitution to hinder its rotation, is free to extend itself smoothly away from the metal and reaction proceeds with an enhanced rate as a result of dinuclear intermediate formation.

Conclusions

The present study has found that for the formation reaction a shift in the rate-limiting step from initial bond formation to second bond formation (ring closure) occurs. The rate of this ring closure is considerably larger for DMEDDA than for the simple amino acids glycine and sarcosine and is attributed to the need for very little rearrangment and rotation prior to ring closure. This rotational barrier has been measured and reflects a modest increase due to the presence of the N-methyl group in DMEDDA as compared to the rotational barrier present in the reactions of nickel(II) with trien and TKED. In contrast, the ICB rate enhancments of glycine and sarco-

sine are larger than the ICB contribution of DMEDDA. The effectiveness of ICB participation is not only dependent upon the relative basicity of the donor group, but also upon the structural environment of the donor group; with tertiary donors being the least effective.

The metal exchnge reaction was found to have a zero-order dependence in copper. DMEDDA may lack the ablity to unwrap from nickel and twist into a conformation suitable for bonding to copper(II) prior to the rate-limiting step.

Suggestions For Further Study

The formation reaction between $Ni(H_2O)_6^{2+}$ and EDDA needs to be studied to allow an accurate determination of the steric effect of the N-methyl group. It would also be interesting to study the metal exchange reaction of N-methylethylenediaminediacetatonickelate(II) with copper(II) ion to see if it also has a zero-order dependence in copper.

REFERENCES

1. Wilkins, R. G.; Eigan, M. "Mechanisms of Organic Reactions," Advances in Chemistry Series, No. 49 American Chemical Society, Washinton D.C., 1965, p. 50ff.

2. Eigan, M. IUPAC 7th International Conference on Coordination Chemistry, Butterworth and Co. LTD., London, 1963.

3. Basolo, F.; Pearson, R. G. "Mechanisms of Inorganic Reactions." John Wiley and Sons, Inc., New York, N.Y., 1958, chapter 3.

4. Eigan, M. in "Advances in the Chemistry of the Coordination Compounds," S. Kirschner, Ed., The MacMillan Co., New York, N.Y., 1961, p. 373.

5. Wilkins, R. G. Accounts of Chem. Res. 1970, 3, 408.

6. Eigan, M.; Kruse, W.; Maass, G.; de Maeyer, L. Progr. Reaction Kinetics 1961, 2, 287.

7. Hammes, G. C.; Steinfeld, J. I. J. Am. Chem. Soc. 1969, 84, 4639.

8. Pearson, R. G.; Ellgen, P. Inorg. Chem. 1967, 6, 1379.

9. Rorabacher, D. B. Inorg. Chem. 1966, 5, 1891.

10. Jones, J. P.; Billo, E. J.; Margerum, D. W. J. Am. Chem. Soc. 1970, 92, 1875.

11. Hunt, J. P. Coord. Chem. Rev. 1971, 7, 1.

12. Turan, T. S.; Rorabacher, D. B. Inorg. Chem. 1972, 11, 288.

13. Rorabacher, D.B.; Turan, T. S.; Defever, J. A.; Nickels, W. G. Inorg. Chem. 1969, 8, 1498.

14. Cassatt, J. C.; Wilkins, R. G. J. Am. Chem.Soc. 1968 90, 6045.

15. Steinhaus, R. K.; Amjad, Z. Inorg. Chem. 1973, 12, 151.

16. Margerum, D. W.; Rorabacher, D. B.; Clark Jr., J. F. G. Inorg. Chem. 1963, 2, 667.

17. Rorabacher, D. B.; Melendez-Cependa, C. A. J. Am. Chem. Soc. 1971, 93, 6071.

18. Turan, T. S. Inorg. Chem. 1974, 13, 1584.

19. Rorabacher, D. B.; Moss, D. B. Inorg. Chem. 1970, 9, 1314.

20. Margerum, D. W.; Cayley, C. W.; Weatherburn, D. C.; Pagenkopf, G. K. "Coordination Chemistry," Mattell, A. E., Ed., American Chemical Society, Washington, D.C., 1978, ACS Monogr. 174, p. 83.

21. Bydalek, T. J.; Margerum, D. W. J. Am. Chem. Soc. 1961, 83, 4326.

22. Margerum, D. W.; Bydalek, T. J. Inorg. Chem. 1962, 1, 852.

23. Bydalek, T. J.; Margerum, D. W. Inorg. Chem. 1963, 2, 678.

24. Margerum, D.W.; Bydalek, T. J. Inorg. Chem. 1963, 2, 683.

25. Bydalek, T. J.; Blomster, M. L. Inorg. Chem. 1964, 3, 667.

26. Bydalek, T. J.; Constant, H. Inorg. Chem. 1965, 4, 883.

27. Margerum, D. W.; Jones, D. L.; Rosen, H. M. J. Am. Chem. Soc. 1965, 87, 4464.

28. Margerum, D. W.; Zabin, B. A.; Janes, D. L. Inorg. Chem. 1966, 5, 250.

29. Margerum, D. W.; Menardi, D. J.; Janes, D. L. Inorg. Chem. 1967, 4, 283.

30. Smith, G. F.; Margerum, D. W. Inorg. Chem. 1969, 8, 135.

31. Steinhaus, R. K.; Swann, R. L. Inorg. Chem. 1973, 12, 1855.

32. Steinhaus, R. K. Inorg. Chem. 1982, 21, 4084.

33. Steinhaus, R. K. to be submitted for publication.

34. Good, N. E.; Winget, G. D.; Winter, W.; Connolly, T. N.; Izawa, S.; Singh, R. M. M. Biochem. 1966, 5, 467.

35. Magee, R. J.; Mazurek, W.; O'Connor, M. J.; Phillip, A. T. Aust. J. Chem. 1974, 27, 1885.

36. "Nuclear Magnetic Resonance Spectra," Spectra No. 8232M, Sadlter Research Laboratories, Inc., Philadephia Pa.

37. Martell, A. E.; Smith, R. M. "Critical Stability Constants," Vol. 1, Plenum Press: New York, N.Y., 1979.

38. Margerum, D. W.; Cayley, C. W.; Weatherburn, D. C.; Pagenkopf, G. K. "Coordination Chemistry," Mattell, A. E., Ed., American Chemical Society, Washington, D.C., 1978, ACS Monogr. 174, p. 133.

39. Margerum, D. W.; Cayley, C. W.; Weatherburn, D. C.; Pagenkopf, G. K. "Coordination Chemistry," Mattell, A. E., Ed., American Chemical Society, Washington, D.C., 1978, ACS Monogr. 174, p. 33-43

40. Margerum, D. W.; Cayley, C. W.; Weatherburn, D. C.; Pagenkopf, G. K. "Coordination Chemistry," Mattell, A. E., Ed., American Chemical Society, Washington, D.C., 1978, ACS Monogr. 174, p. 5.

41. Hoffmann, H.; Bunsenges, H. Ber. Phys. Chem. 1969, 73, 432.

42. Steinhaus, R. K.; Kolopajlo, L. H. submitted for publication.

43. Pasternack, R. F.; Kustin, K.; Hughes, L. A.; Gibbs, E. J. Am. Chem. Soc. 1969, 91, 4401.